

Investigating the Link between Space-Weather Parameters and Forbush Decrease

^{1,2}Nwuzor, O. C., ³Okike, O., ⁴Okpara, P. A., ^{1,5}Chikwendu, A. O.,
²Ekweh, A. K. and ³Akande, P. I.



¹Department of Industrial and Medical Physics, David Umahi Federal University of Health Sciences, Uburu

²Directorate of Launch Services and Space Operations, Defence Space Administration, Abuja

³Department of Industrial Physics, Ebonyi State University, Abakaliki

⁴Department of Industrial Mathematics and Health Statistics, David Umahi Federal University of Health Sciences, Uburu

⁵International Institute of Oncology and Cancer Research, David Umahi Federal University of Health Sciences, Uburu

*Corresponding author's email: nwuzorogoo@gmail.com

ABSTRACT

The link between space-weather parameters and Forbush decrease has been investigated. The aim was to determine the relationship between space-weather parameters and forbush decrease. Daily cosmic ray counts from MGDN station for 2010-2015 were used to achieve this aim. Solar wind speed (SWS) and interplanetary magnetic field (IMF) intensity were equally used as space-weather parameters. The semi-automated method of FD detection was deployed. This method generated 1104 FDs for the MGDN station within the years under study. A correlation and regression between FDs and space-weather parameters (SWS and IMF) were further tested. The results of the correlation and regression are statistically significant. The implications of the present space-weather data on FDs are highlighted.

Keywords:

Cosmic rays,
Galactic cosmic rays,
Forbush decreases,
Interplanetary magnetic field,
Solar wind speed.

INTRODUCTION

Forbush decreases (FDs) are short-term variations in the intensity of galactic cosmic rays (Alhasan *et al.*, 2021). This event in some instances, are regarded as a rapid and transient decrease in GCR intensity to the tune of 2%-30% (Belov, 2009). The fundamental idea behind FDs is traced to the work of an American Physicist, Scott E. Forbush (Forbush, 1938). FDs are generally classified into recurrent and non-recurrent FDs. While recurrent FDs are caused by corotating high-speed solar wind streams (CSWSs) from coronal holes (CHs) which corotate with the Sun (Alhasan *et al.*, 2021), non-recurrent FDs are caused by the coronal mass ejections (CMEs) and their interplanetary counterparts, interplanetary coronal mass ejection (ICMEs) (Alhasan *et al.*, 2021). On a general note, solar wind disturbances in the form CMEs, ICMEs, corotating interacting regions (CIRs) and CSWS structures is the determinant for cosmic ray (CR) intensity depressions on Earth (Okike and Nwuzor, 2020).

However, since the discovery of FD, numerous research has discussed the phenomenon, while the origin and its connection with space-weather structure remain a

subject of serious debate (Okike and Nwuzor, 2020). Previous research reported the association of fd amplitude with the interplanetary magnetic field (imf), solar wind speed (sws) and geomagnetic disturbance storm time (dst) (Cane *et al.*, 1993; Belov, 2009; Belov *et al.*, 2001a; Lingri *et al.*, 2016; Okike and Nwuzor, 2020; Alhassan *et al.*, 2021). It is noted that FDs and geomagnetic storms are both traced to the disturbances in the interplanetary medium (Belov *et al.*, 2021a). Similarly, solar wind disturbances, magnetosphere and FDs are activated by the same solar process (Alhassan *et al.*, 2021). However, the investigation of these disturbances is paramount in comprehension of the dynamics of the solar-terrestrial environment since they pose potential risk of life-threatening issues ranging from satellite damage, communication failure to navigational difficulties (Joselyn and McIntosh, 1981; Rathore *et al.*, 2011). Thus, the need for the investigation of the relationship between solar-geomagnetic characteristics and GCR intensity reduction.

MATERIALS AND METHODS

The major materials used for this research are the daily CR intensity counts that was obtained from <http://cr0.izmiran.ru/common/> for Magadan (MGDN) CR station. The cutoff rigidity of the station is 2.11GV with coordinates of 60.12°N, 151.02°E and an altitude of 220m. The data of solar wind speed (SWS) and interplanetary magnetic field (IMF) were also used and sourced from <https://omniweb.gsfc.nasa.gov/html/owdata.html> for the same period under study. These data covered the period of six years between the years 2010 to 2015. R. Statistical software and a laptop computer were equally used for the statistical analysis.

Data harvesting

The daily data of cosmic rays were sourced from the Izmiran website for all thirteen cosmic ray stations and the period under study. These daily data were placed and arranged in a text editor software. The 00 hours as contained in the raw data were filtered off from the CR data since we are working with daily counts. The data after arrangement contains only the dates and the CR counts in a well-arranged tabular form. They were further saved with a unique file name for each neutron station. In addition, the solar wind speed (SWS) and interplanetary magnetic field data were also sourced from the internet and arranged in a tabular form. The data covers the same period as that of CR. They were filtered to the tune of dates and counts on the process of the download using the website data query. They were also further saved with unique fine names.

Data Processing

The semi-automated method of FD selection was used in this work. This method involves the use of computer software program that is operated using R. statistical software. The method of program FD event location developed by Okike and Umahi (2019b) was employed

in the present investigation. The processes and stages involved in this method are as explained below;

(a) The program restructured the raw CR data into a unique nature of dates and counts. It further saves same with a unique fine name.

(b) The program read the file as saved in (a) above, scale and plot the daily variations of the CR counts for the period under study.

(c) The program normalized the daily CR counts using

$$CR(\%) = \frac{CR - CR_q}{CR_q} \times 100\% \quad (1)$$

(d) It further plotted the normalized CR counts with dates. This indicated decreases in the variations of CR counts by giving a baseline for FD detection using an abline along the CR variations.

(e) A threshold of $< -0.5\%$ was used as a baseline for FD magnitude selection

(e) The program then filtered the observed variation for the first time using a red plotted points.

(f) It further filtered the variations for the second time by feeding the program with the identified FD dates and magnitudes to indicate a clearer point of FDs in the third plot.

The list of FD dates and magnitudes was presented. The FD magnitudes were presented as an FD catalog. The corresponding SWS and IMF data were equally placed side by side with the FDs and presented in a tabular form. Correlation and regression were tested between some selected FD magnitudes and and space-weather parameters (SWS and IMF).

RESULTS AND DISCUSSION

The results of this research are presented in accordance with the methods applied. Firstly, Figure 1a and 1b depicts the variations of raw cosmic ray intensity daily counts while Figure 2a and 2b show the filtration of the CR daily counts which indicate a clear view of the points of CR depression.

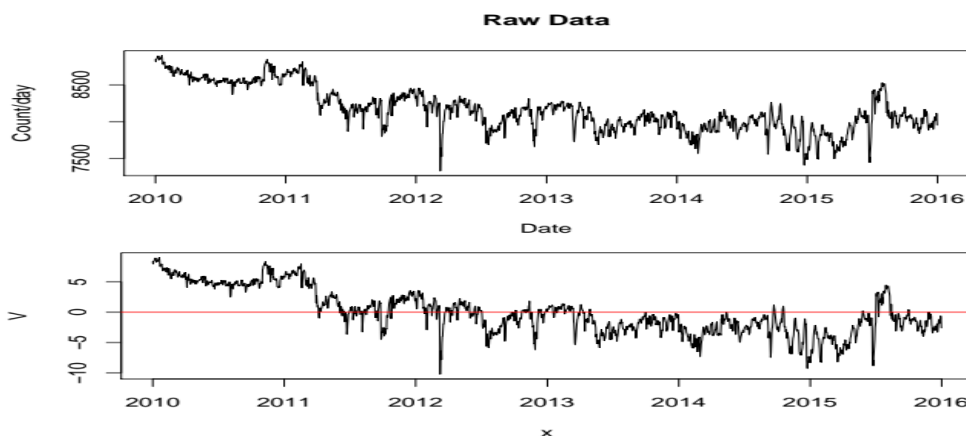


Figure 1: (a) Variations of cosmic ray raw data. (b) Variations of cosmic ray raw data showing a baseline for FD selection

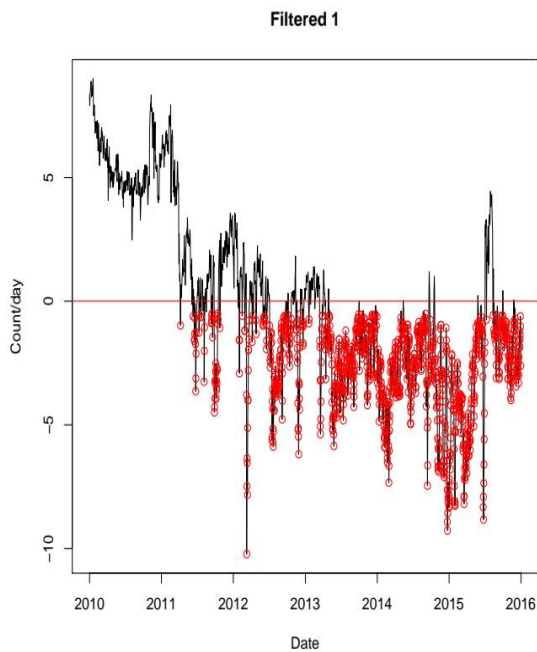


Figure 2(a): First filtration of FDs

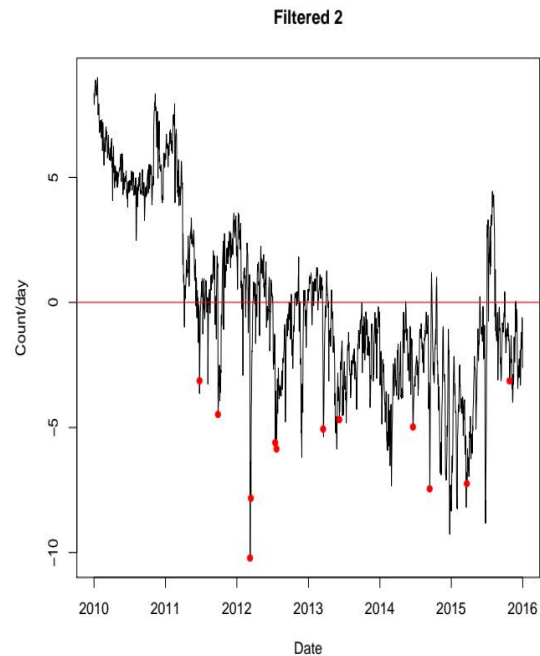


Figure 2(b): Second filtration of FDs

The results of this research are presented by the methods applied. Firstly, Figure 1a and 1b depicts the variations of raw cosmic ray intensity daily counts while Figure 2a

and 2b show the filtration of the CR daily counts which indicate a clear view of the points of CR depression.

Table 1: Selected FD dates and magnitudes from MGDN CR station

S/NO	DATE	FD MAG (%)	SWS	IMF
1	2011-04-08	-0.98	430	4.6
2	2011-06-11	-0.61	403	7.5
3	2011-06-17	-1.53	470	7.2
4	2011-06-18	-1.61	415	4.8
5	2011-06-19	-1.31	396	4.5
6	2011-06-20	-0.69	395	5.2
7	2011-06-23	-1.73	605	7.1
8	2011-06-24	-3.64	610	4
9	2011-06-25	-3.12	583	3.8
10	2011-06-26	-2.12	528	3.4
11	2011-06-27	-1.27	445	3.2
12	2011-07-11	-1.26	520	7.5
13	2011-07-12	-0.56	681	4.1
14	2011-07-20	-0.61	625	5.6
15	2011-07-21	-0.65	685	4
16	2011-08-06	-3.26	535	10.3
17	2011-08-07	-2.01	539	4.4
18	2011-08-08	-1.05	548	4.3
19	2011-09-11	-0.88	597	5.7
20	2011-09-12	-0.76	617	5.7
21	2011-09-13	-0.56	579	5.6
22	2011-09-14	-0.86	518	3.1
23	2011-09-15	-0.5	458	3.5
24	2011-09-18	-1.46	441	6.5
25	2011-09-26	-0.71	462	13.5
26	2011-09-27	-4.5	604	6.7

27	2011-09-28	-4.28	486	4.6
28	2011-09-29	-3.93	539	5.3
29	2011-09-30	-3.21	454	4.5
30	2011-10-01	-3.32	495	4.6
31	2011-10-02	-3.21	488	4
32	2011-10-03	-2.82	399	4.1
33	2011-10-04	-2.51	359	4.8
34	2011-10-05	-2.89	420	9.1
35	2011-10-06	-3.93	376	10.4
36	2011-10-07	-3.52	375	3.8
37	2011-10-08	-3.22	351	4.4
38	2011-10-09	-3.59	333	6.7
39	2011-10-10	-3.33	343	5.4
40	2011-10-11	-2.71	364	5.4
41	2011-10-12	-2.79	392	5.3
42	2011-10-13	-0.59	359	5
43	2011-10-14	-0.5	381	6.3
44	2011-10-15	-0.91	444	6.8
45	2011-10-16	-0.74	451	4.9
46	2011-10-25	-1.08	484	16.9
47	2012-01-31	-1.57	363	5.8
48	2012-02-01	-2.92	380	6.5
49	2012-02-02	-1.57	408	4.8
50	2012-02-15	-0.59	381	8.6

The Pearson correlation approach was used to test for correlations between FDs and space-weather parameters (SWS and IMF). The general Pearson correlation formula is;

$$r = \frac{\sum_{j=1}^k (x_j - \bar{x})(y_j - \bar{y})}{\sqrt{\sum_{j=1}^k (x_j - \bar{x})^2 \sum_{j=1}^k (y_j - \bar{y})^2}} \quad (2)$$

(Okwonu *et al.*, 2020)

Where r = correlation coefficient, $\bar{x} = \frac{\sum_{j=1}^k x_j}{k}$ and $\bar{y} = \frac{\sum_{j=1}^k y_j}{k}$ are the sample means. Note that $(x_j, y_j, j = 1, \dots, n)$ are data points from two variables assumed to be normally distributed with parameters $\mu^x, \mu^y, \delta_{\mu^x}^2, \delta_{\mu^y}^2$.

The results of these correlations are shown with table 2 and plots of Figures 3 and 4.

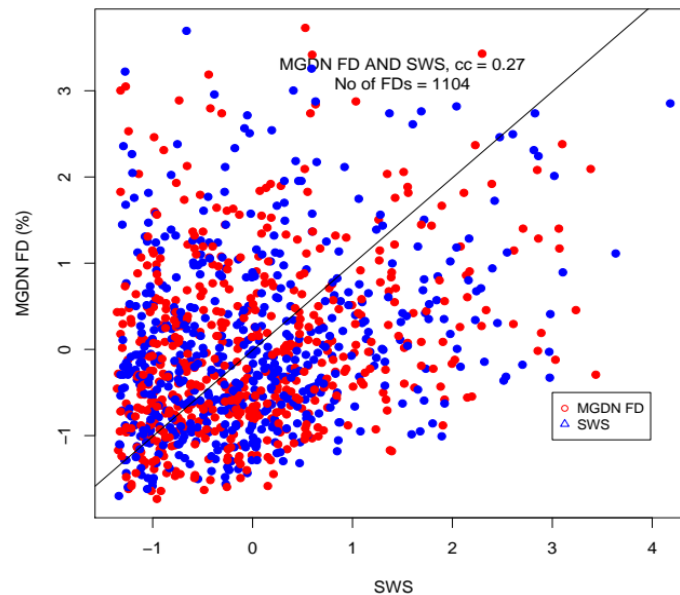


Figure 3: Correlation results of MGDN FDs and SWS

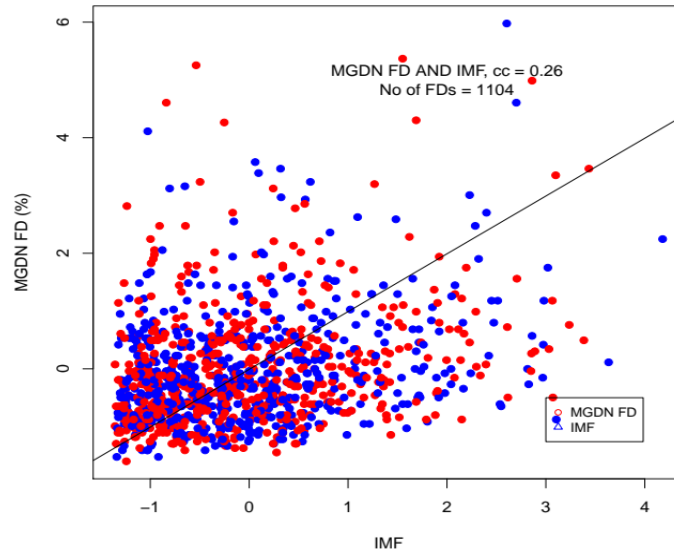


Figure 4: Correlation plot of MGDN FDs and IMF

Table 2: Correlation results of MGDN FDs with SWS and IMF

FD vs SWS	FD vs IMF
0.27	0.26

The regression between FD magnitudes of MGDN CR stations is and space-weather parameters (SWS and IMF) are as presented below. Generally, the regression equations are of the form;

$$y = c + mx \tag{2}$$

Where c = intercept, m = slope

The result of the regression analysis between FD magnitudes with SWS is shown in Figure 5. Similarly, the regression equation is given as;

$$FD_{MGDN} = 381.58 \pm 4.82 + (13.48 \pm 1.43) FD_{SWS} \tag{3}$$

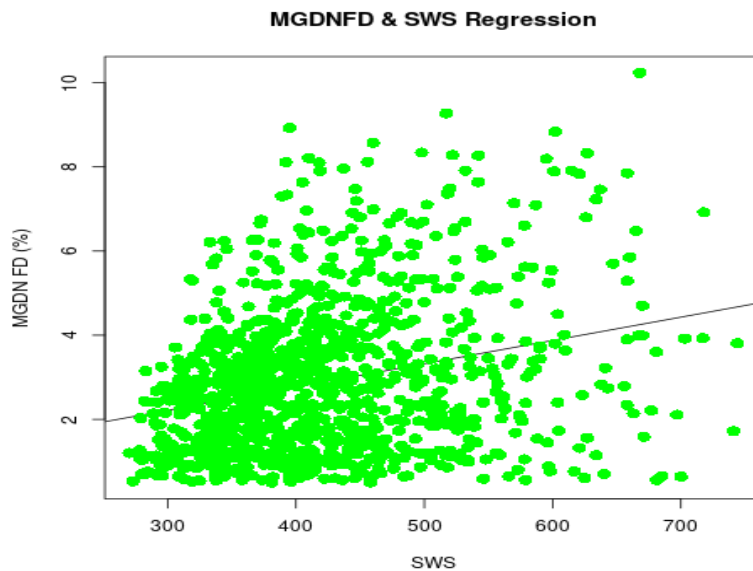


Figure 5: Regression plot of MGDN FD and SWS

The result of the regression analysis between FD magnitudes with IMF is shown in Figure 6. Similarly, the regression equation is given as;

$$FD_{MGDN} = 4.97 \pm 0.14 + (0.39 \pm 0.04) FD_{IMF} \tag{4}$$

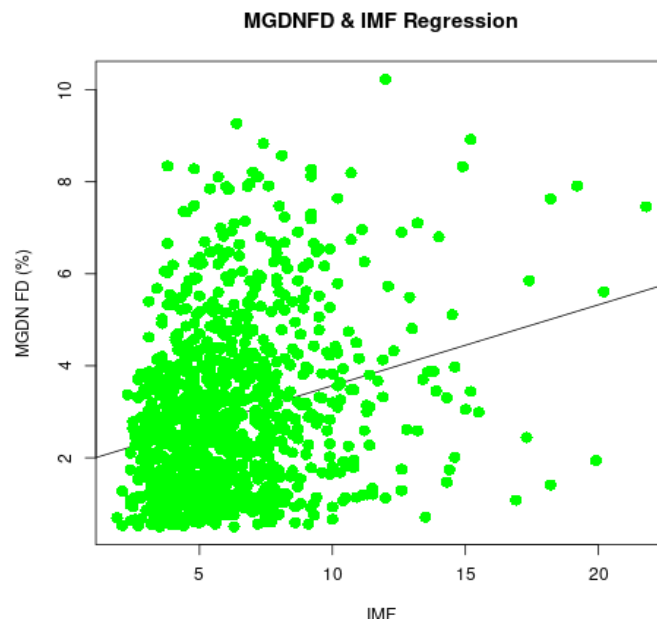


Figure 6: Regression plot of MGDN FD and IMF

Discussion

The semi-automated method of FD selection used in this work detected 1104 FDs for the MGDN station. These FDs were used to form a catalog of FD and the sample was presented in Table 1, we found a connection between FD versus SWS, and FD versus IMF. Research has shown a correlation between FD magnitude and solar activities such as solar wind and interplanetary magnetic field. Belov *et al.* (2001) revealed that the correlation between FD magnitude and the product of the magnetic field enhancement and the SW speed increase is better than correlations for the two SW parameters treated separately. Therefore, we analyzed correlations of FD magnitudes with the solar wind speed (SWS) and interplanetary magnetic field (IMF) data to test which of these solar parameters is the most relevant to FDs. Table 2 shows the correlation between FD magnitudes of the MGDN station for the period under study with SWS and IMF. From the analysis, the FDs of the MGDN station recorded the correlation coefficients of $cc = 0.27$ with SWS, and a correlation coefficient of $cc = 0.26$ with IMF. It was observed that solar wind had a stronger correlation with the FD magnitudes than the IMF. This signifies that solar wind disturbances have greater tendencies to cause FDs when compared to the IMF. Figures 3 & 4 show the correlation plot of MGDN FD with SWS and IMF respectively. The alignment of the scattered points along the line of best fit is a clear indication of good correlation, which signifies a relationship between FDs, SWS and IMF. However, several other parameters such as CME speed or transit speed, magnetospheric effects, sunspot number, current sheet tilt angle, solar magnetic turbulence level, CR anisotropy, heliospheric magnetic sector, rigidity,

differences in the local time of the two stations, instrumental variations and so on, which affect CR time-intensity variations, should also be tested before reaching any definitive conclusion on the extent of the relationship between FDs and solar parameters (Cliver and Cane, 1996; Singh ET AL., 1997; Smith, 1990; Wibberenz ET AL., 2001; Owens ET AL., 2014; Okike 2019, 2020a; Okike and Nwuzor, 2020). In some past articles that analyzed the relationship between FDs and these physical parameters, the magnitude and timing of Forbush events were manually estimated. The present large event catalog is an indication that only FD subsamples (see Laken ET AL., 2012, for a detailed discussion on the bias implications of a small sample of FD events) were employed in some of the previous submissions that manually calculated FD event magnitude and timing (Barouch and Burlaga, 1975; Richardson, 2004; Kane, 2010).

To further test the connection between FDs and solar parameters, a regression was tested between the FDs with SWS and IMF. The results of the regression are shown in Figures 6 & 7 and equations (3) and (4) respectively. The R^2 , r and associated p-values for all the events at MGDN (Figure 6 and 7) are 0.07, 0.12 and 0.14, -0.36 , -0.35 and -0.37 , and 3.16×10^{-8} , 8.53×10^{-8} and 5.37×10^{-6} respectively. The regression all show a high level of significance at the 95% confidence level. This agrees with Okike *et al.*, (2021b) which found FD versus IMF correlation coefficient $r \sim -0.34$ statistically significant at the 90% significance level. This finding was based on strong FDs selected using a large $CR(\%) \leq -3$ baseline. The present regression analysis result compares favourably with their finding. This is consistent with the fact that enhanced IMF

hinders CR intensity propagation to the Earth and thus results in high-magnitude FD detection (Lingri *et al.*, 2016).

CONCLUSION

The study of solar-weather parameters responsible for the variations of GCR on Earth remains a subject of research interest. Many research on this subject employ correlation and regression statistical approaches to find the possible link between FDs and space-weather. FD selection as a key parameter is very important in the study of solar-terrestrial connection. Many investigators employ manual methods in identifying FDs. In this work, we have deployed a semi-automated method to both calculate the amplitude of FDs as well as detecting the number of FDs that occurred between 2010-2015. The FD method employed here is capable of selecting FD magnitude of -0.5% . The correlation and regression results demonstrate that there were significant space-weather disturbances at the time of the CR flux depressions. All the relations are statistically highly significant. Other factors than IMF, SWS were equally reviewed to may have control the amount of CR flux arriving at Earth. The observed high statistical significance of the correlation between FDs, solar wind data and geophysical parameters could imply that SWS and IMF intensity have the same causative agent since their impact on GCR intensity variations is significant.

REFERENCES

Alhassan J. A., Okike O and Chukwude A. E. (2021). Investigation of the relation between space-weather parameters and Forbush decreases automatically selected from Moscow and Apatity cosmic ray stations during solar cycle 23. *Research in Astronomy and Astrophysics*, 21(11), 273.

Barouch, E., and Burlaga, L. F. (1975). Causes of Forbush decreases and other cosmic ray variation. *J. Geophys. Res.*, 80, 449

Belov, A., (2009). Universal heliophysical processes. In: Proceedings of the International Astronomical Union. *IAU Symposium*, 257, 439–450

Belov A. V., Eroshenko E. A., Oleneva V. A., Struminsky A. B., and Yanke V. G. (2001). What Determines the Magnitude of Forbush Decrease? *Adv. Space Res.*, 27(3), 625-630.

Cane, H. V., Richardson, I. G., von Roseninge, T. T., and Wibberenz, G. (1993). Cosmic ray decreases and shock structure: A multispacecraft study. *JGR*, 99(11), 21429-21441

Cliver, E. W., and Cane, H. V. (1996). The angular extents of solar/interplanetary disturbances and modulation of galactic cosmic rays. *J. Geophys. Res.*, 101, 15533

Forbush S. E., (1938). On the effects in cosmic-ray intensity observed during the recent magnetic storm. *Physical Review*, 51(12), 1108–1109.

Joselyn, J.A. and McIntosh, P.S. (1981). Disappearing solar filaments: A useful predictor of geomagnetic activity. *Journal of Geophysical Research* 86, 4555. doi: 10.1029/JA086iA06p04555. Issn: 0148-0227.

Kane, R.P., (2010). Severe geomagnetic storms and Forbush decreases: interplanetary relationships re-examined. *Ann. Geophys.*, 28, 479–489.

Laken, B. A., Pallé, E., Čalogović, J., and Dunne, E. M. (2012). A cosmic ray-climate link and cloud observations. *Journal of Space Weather and Space Climate*, 2, A18

Lingri, D., Mavromichalaki, H., Belov, A., Eroshenko, E., Yanke, V., Abunin, A., and Abunina, M. (2016). Solar activity parameters and associated Forbush decreases during the minimum between Cycles 23 and 24 and the ascending phase of Cycle 24. *Solar Phys.*, 291(3), 1025.

Okike O. (2019a). Chree Method of Analysis: A Critique of Its Application to Forbush Events Selection Criteria and Timing. *APJ*, 882, 15

Okike, O., Umahi, A.E. (2019). The Empirical Implication of Conducting a Chree Analysis Using Data from Isolated Neutron Monitors. *Sol Phys*, 294, 16 <https://doi.org/10.1007/s11207-019-1405-y>

Okike O. (2020). Automated detection of simultaneous/non-simultaneous Forbush decreases and the associated cosmic ray phenomena, *Journal of Atmospheric and Solar-Terrestrial Physics*, 211,1364-6826

Okike O. and Nwuzor O. C. (2020). Investigation of the rigidity and sensitivity dependence of neutron monitors for cosmic ray modulation using algorithm-selected Forbush decreases. *MNRAS*, 493, 1948–1959.

Okike, O., Alhassan, J, Iyida E. and Chukwude, A. E. (2021). A comparison of catalogues of Forbush decreases identified from individual and a network of neutron monitors: a critical perspective. *Monthly Notices of the Royal Astronomical Society*. 503. 5675-5691. 10.1093/mnras/stab680.

Owens, M. J., Scott, C. J., Lockwood, M., Barnard L., Harrison R. G., Nicoll K., Watt C., Bennet A. J. (2014). Modulation of UK lightning by heliospheric magnetic field polarity. *Environmental Research Letters*, 9, 115009

Rathore, B.S., Kaushik, S.C., Firoz, K.A., Gupta, D.C., Shrivastva, A.K., Parashar, K.K. and Bhadoria, R.M. (2011) A Correlative Study of Geomagnetic Storms Associated with Solar Wind and IMF Features During Solar Cycle-23. *International Journal of Applied Physics and Mathematics*, 1, 149-154. <http://dx.doi.org/10.7763/IJAPM.2011.V1.29>

Richardson, I. G. (2004). The fraction of interplanetary coronal mass ejections that are magnetic clouds:

Evidence for a solar cycle variation. *Geophysical Research Letters*, 31 (18). doi:10.1029/2004gl020958

Singh, M., Nigam, S. K., and Shrivastava, P. K. (1997). Long-term cosmic ray intensity variation in relation with new modulation parameter $\sim 1 \sim 2$. *Asian Journal Of Physics* 6, 473-475

Smith, E. J. (1990). Magnetic Fields in the Heliosphere: Pioneer Observations. *J. Geophys. Res.*, 95, 18731

Wibberenz, G., Cane, H. V., Richardson, I. G., and Von Roseninge, T. T. (2001). The Influence of Tilt Angle and Magnetic Field Variations on Cosmic Ray Modulation. *Space Science Reviews*. 97. 343-347